Polymer Testing 121 (2023) 107983

Contents lists available at ScienceDirect

Polymer Testing

journal homepage: www.elsevier.com/locate/polytest

A study on miscibility properties of polyacrylonitrile blending films with biodegradable polymer, shellac

Beom-Gon Cho [a,b,c,1,*], Jung-Eun Lee [a], Seung-Yeol Jeon [b,**], Han Gi Chae [a,***]

[a] School of Materials Science and Engineering, Ulsan National Institute of Science and Technology (UNIST), UNIST-gil 50, Ulju-gun, Ulsan, 44919, Republic of Korea
[b] Carbon Composite Materials Research Center, Institute of Advanced Composite Materials, Korea Institute of Science and Technology (KIST), 92 Chudong-ro, Bongdong-eup, Wanju-gun, Jeollabuk-do, 55324, Republic of Korea
[c] Chemical Materials R&D Department, Chassis & Materials Research Laboratory, Korea Automotive Technology Institute (KATECH), 303 Pungse-myeon, Dongnam-gu, Cheonan-si, Chungcheongnam-do, 31214, Republic of Korea

ARTICLE INFO

Keywords:
Polyacrylonitrile
Shellac
Polymer blending
Compatibility
Hydrogen bonding
Mechanical performance

ABSTRACT

Polyacrylonitrile (PAN) films blended with shellac, biodegradable polymer, were prepared via simple solution casting method. The miscibility of PAN with shellac polymer was investigated and the optimal concentration of shellac in terms of hydrogen bonding between shellac and PAN chain was determined to be used as a novel biomass carbon precursor. Shellac and PAN chain could exert interaction and the interaction facilitates to loose the crystalline structure of the PAN chain, suggesting that the decrease of the oxidation temperature of the PAN chain in the PAN/shellac blends film by the introduction of shellac segments. The optimal PAN/shellac blends film exhibited outstanding mechanical performances (73.8% higher tensile strength, 60% higher storage modulus compared with control PAN film) showing homogeneous blending state.

1. Introduction

In recent years, polymer blending has become the most useful way to improve or modify the physicochemical properties of polymer materials [1–5]. An important property of polymer blends is the miscibility of the ingredients. This is because it affects the mechanical properties, morphology, permeability and degradation of the polymer blends. Numerous investigations regarding the miscibility in multi-component polymer systems have been reported [6–9]. Among them, polymer blends between biopolymers and synthetic polymers are particularly important as they can be used as biomedical and biodegradable materials [3,5,10–13]. Therefore, many studies are being conducted because the miscibility of each component polymer is quite important to open up the feasibility of the application. One of the influencing factors of thermodynamic miscibility is interchain hydrogen bonding or van der Waals attraction. Recently, environmental issues for non-biodegradable polymers such as polyacrylonitrile (PAN) and polyester are starting to receive great attention from the viewpoint of changing their physicochemical properties in various ways. PAN has good mechanical property and hydrophobicity and has been widely used as precursor materials for carbon fiber manufacturing as well as film materials [14–17]. In addition, it is expected that the physicochemical properties of the PAN film can be controlled by introducing a biopolymer into the PAN film.

Meanwhile, shellac is a pale yellow carbon-based natural polymer resin obtained from the secretions of laccifer lacca, a caterpillar that lives in India and Thailand. The worldwide production of shellac is estimated at around 50,000 tons/year, making it an inexpensive bio-raw material at just $2/kg. Therefore, it is an important renewable resource that cannot be ignored for bio-based long-chain polyhydroxyesters [18–21]. Shellac is a natural polymer that contains hexagonal and penta-membered carbon rings and has a structure in which a hydroxyl group and a carboxyl group are bonded to an aliphatic carbon chain [21–23]. Interestingly, as shellac undergoes heat treatment, dehydration reaction proceeds at a temperature of 150 °C or higher, resulting in the

* Corresponding author. Chemical Materials R&D Department, Chassis & Materials Research Laboratory, Korea Automotive Technology Institute (KATECH), 303 Pungse-myeon, Dongnam-gu, Cheonan-si, Chungcheongnam-do, 31214, Republic of Korea.
** Corresponding author.
*** Corresponding author.
E-mail addresses: bgcho@katech.re.kr (B.-G. Cho), syjeon@kist.re.kr (S.-Y. Jeon), hgchae@unist.ac.kr (H.G. Chae).
[1] Present Addresses The first author, Beom-Gon Cho is now in the Korea Automotive Technology Institute (KATECH) after moved from Korea Institute of Science and Technology (KIST) and Ulsan National Institute of Science and Technology (UNIST) past.

https://doi.org/10.1016/j.polymertesting.2023.107983
Received 7 November 2022; Received in revised form 16 February 2023; Accepted 8 March 2023
Available online 12 March 2023

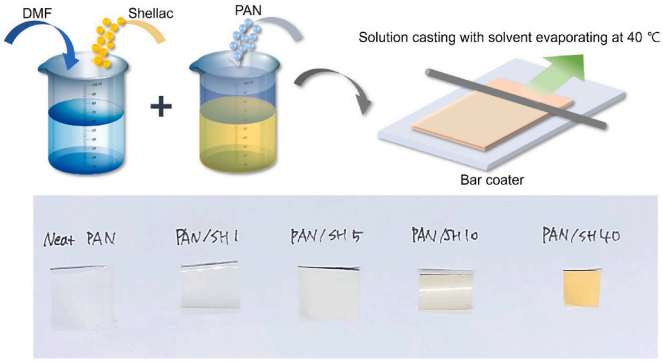

Fig. 1. Overall process of preparation of PAN/shellac film via solution casting method, and photographs of resultant film with different shellac concentration.

Table 1
Sample codes.

Sample code	PAN wt.%	Shellac wt.%
Neat PAN	100	0
PAN/SH1	99	1
PAN/SH5	95	5
PAN/SH10	90	10
PAN/SH40	60	40

breakdown of ester and aldehyde bonds and decomposition into mono-molecules of hydrocarbons such as methyl and ethyl together with water vapor. At a high temperature of 500 °C or higher, as the bond rearrangement occurs in which the hydroxyl group of the aliphatic compound is removed, graphene oxide (GO) with a sp^2 hybridized carbon network structure is gradually formed [19,21,22,24]. Meanwhile, the formation of hydrogen bonds between PAN segments and shellac chains could promote the miscibility of PAN and shellac [9,18,25,26]. However, to the best of our knowledge, no experimental studies on the properties of PAN/shellac blend films have been reported so far.

Herein, the blending optimization between PAN and shellac molecules was performed. The PAN/shellac blends film was prepared by solution casting with different shellac concentration, and before that, the optimal ratio was determined by analyzing the rheological behavior of the PAN/shellac blending solution. In addition, the interaction between the PAN chain and the shellac chain, that is, which chemical bonding exists, was confirmed through FTIR analysis, and crystallinity behavior and thermal decomposition behavior of the blends film were investigated through WAXD, DSC, and TGA. Finally, it could be determined the optimal ratio of shellac to PAN in the blends film through mechanical test such as DMA. The results revealed that the introduction of shellac could exert great effects on the properties of PAN film.

2. Experimental

2.1. Materials

Shellac flakes (dewaxed orange) were provided by Shellac Shack, USA and used as blending materials with homopolymer polyacrylonitrile (PAN) (250,000 g/mol), which was purchased from Sigma-Aldrich, USA. For the fabrication of PAN/shellac blend film, dimethylformamide (DMF, Samchun, Korea) was used as solvent.

2.2. Preparation of PAN-Shellac blend film

Blends of PAN and shellac were prepared through simple solution casting method as shown in Fig. 1. Firstly, the commercial shellac flakes were crumbled to fine powder through ball milling and then dried at 80 °C for overnight in the vacuum oven before using. Likewise, PAN was dried with same condition to shellac. The dried shellac of certain weight percentage was dissolved in 100 mL of DMF with stirring rate of 500 rpm at 60 °C until perfectly dissolved. Subsequently, 12 g of PAN was added to shellac suspension with stirring again. The PAN-shellac solution was cast onto glass using a bar coater to make a film with a thickness of 40 *μm*. The solution was dried at 40 °C in the vacuum oven for 1 day to evaporate DMF. Furthermore, it was treated in distilled water at 80 °C for 2 h and then dried at 40 °C for 1 day to remove the residue solvent perfectly. After the solvent was removed completely, the final resultant film was peeled off, having different shellac concentration from 1 wt% to 40 wt% with respect to blends as listed in Table 1.

2.3. Characterization

Before preparing the PAN-shellac blends film, the rheological properties of the blending solution were analyzed using an oscillatory rheometer (Haake MARS III, Thermo Scientific). The frequency sweep test was performed in the range of 0.05 – 200 rad/s at the 25 °C and constant strain of 5%.

The morphologies of the PAN/shellac blend film were investigated using field-emission scanning electron microscopy (FE-SEM; Nova Nano230, FEI, USA) after platinum coating for 1 min. Furthermore, the nanoscale morphologies of the blends were analyzed using negative staining transmission electron microscopy (TEM; Tecnai G2 spirit twin,

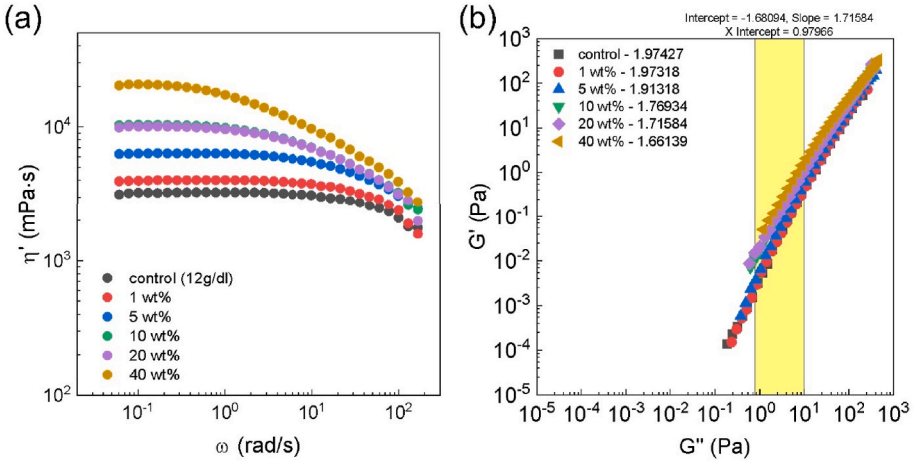

Fig. 2. (a) dynamic viscosity as a function of angular frequency and (b) logarithmic plot of G' versus G'' for PAN/shellac blends solution with different shellac concentration.

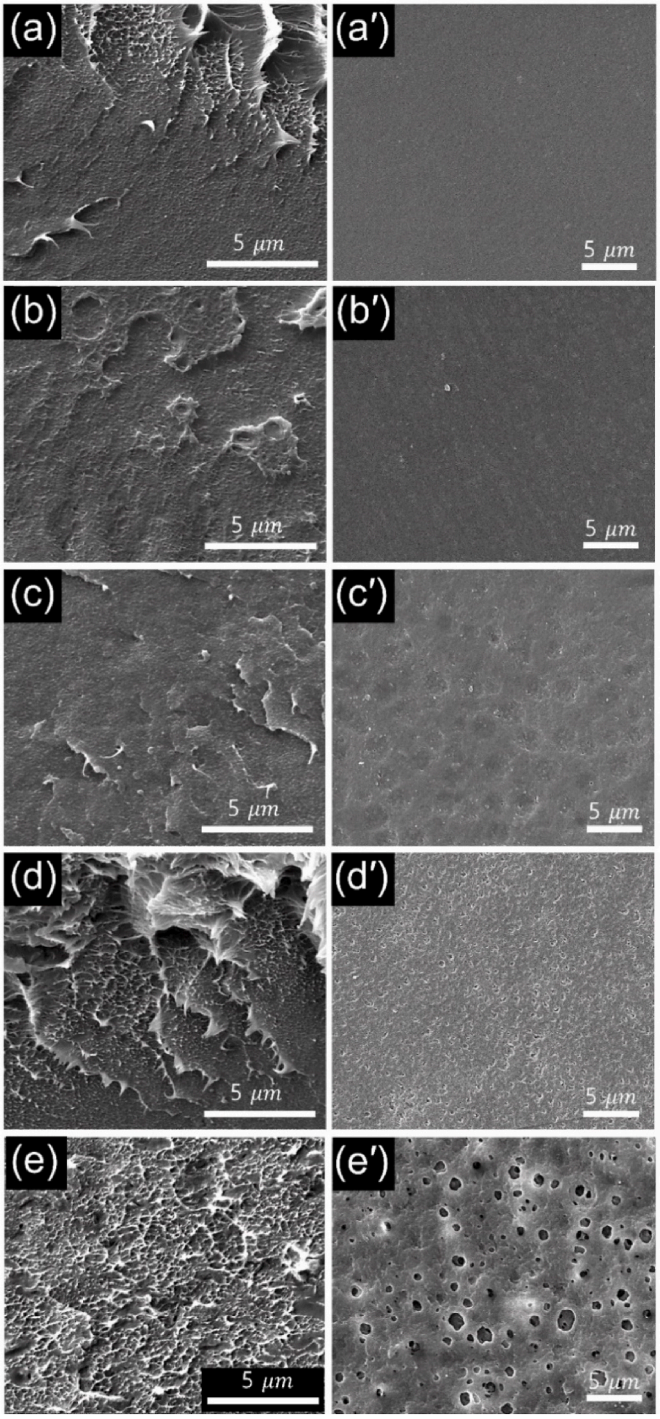

Fig. 3. SEM images of PAN/shellac blends film with different shellac concentration: cross-section (a) 0 wt%; (b) 1 wt%; (c) 5 wt%; (d) 10 wt%; and (e) 40 wt %, respectively, and surface (a') 0 wt%; (b') 1 wt%; (c') 5 wt%; (d') 10 wt%; and (e') 40 wt%, respectively.

FEI, Netherlands) to prove the compatibility of the polymers with 120 kV of accelerating voltage. For sampling to TEM analysis, a 10 μl of PAN/shellac blending solution was over-coated on Ni grid, followed staining for 2 min with 5% of uranyl acetate. After drying them with air for 30 min, the sample finally was prepared for TEM analysis. Meanwhile, to determine the optimal blend ratio, various spectroscopic analyses were thoroughly performed. Fourier-transform infrared (FTIR) spectroscopy was performed using a 670-IR spectrometer (Varian, USA) on sample powders of PAN/shellac film to determine hydrogen bonding in the films. The samples were analyzed in the transmittance mode over the scanning range of 400 − 4000 cm^{-1}. Moreover, wide-angle X-ray diffraction (WAXD) patterns were recorded on a high − resolution X-Ray diffractometer (X'Pert PRO MRD, Panalytical, Netherlands) with Cu Kα radiation ($\lambda = 1.542$ Å) by operating the target at 45 kV and 40 mA. The scanning was performed from 5° to 50° with a rate of 0.3°/min at 25 °C. WAXD analysis was performed on the PAN/shellac blend films to investigate the blending behavior between PAN and shellac chains in the films by calculating the crystallite size of PAN. Meanwhile, the crystallinity of the film was also calculated using the crystallinity index (CI).

Differential scanning calorimetry (DSC, Q200, TA instruments, USA) analysis was carried out under a nitrogen atmosphere with heating from 30 to 400 °C at a rate of 10 °C/min and cooling to 30 °C at a rate of 10 °C/min, and their crystallization exotherms were recorded. The thermal decomposition behavior of the PAN/shellac blend films were estimated using thermogravimetric analysis (TGA, Q50, TA instruments, USA) at a heating rate of 10 °C/min from 30 °C to 650 °C under a nitrogen atmosphere.

The tensile properties of the PAN/shellac blend films having dimensions of 5 mm × 30 mm × 0.03 mm were analyzed using a dynamic mechanical analysis equipment (DMA, Q800, TA Instruments, USA). The measurements were conducted in strain ramp mode using a tension film clamp with a tension rate of 1 mm/min. Furthermore, thermomechanical properties of the PAN/shellac blend films were estimated using DMA. The measurements were performed under the frequency-strain sweep mode using a tension film clamp in the temperature range 30–200 °C at a frequency of 1 Hz and a heating rate of 3 °C/min.

3. Results and discussion

3.1. Rheological behavior of PAN/shellac blend solution

As shown in Fig. 2 (a), as the shellac concentration increases, the dynamic viscosity of the solution increases. It indicates that an interaction between PAN and shellac was induced. Furthermore, the frequency value corresponding to shear thinning behavior also gradually decreased with increases of shellac concentration. Meanwhile, the homogeneity of a solution can be expressed as the slope value of the G' versus G'' log plot (cole-cole plot). The ideal solution has a slope value of 2, and the closer the slope value is to 2, the more uniform the solution. As shown in this Fig. 2 (b), the slope values are comparable from control sample to shellac 5 wt% sample. It means that up to 5 wt% of shellac, it is blended well by the interaction between the shellac and the PAN chain, or the small size of the shellac does not significantly affect to the uniformity of the solution. Beyond the 5 wt%, the uniformity of solution decreases resulting from the aggregation of shellac. Accordingly, the excessive shellac concentration in PAN/shellac blending may cause the deterioration of miscibility resulting in decreasing of physical and mechanical properties of the blends film.

3.2. Morphology of PAN/shellac blend film

The representative SEM images of cross section and surface of the PAN/shellac films with different shellac concentration are shown in Fig. 3. Fig. 3 (a − e) demonstrates the differences of compatibility and blend morphologies. It is clearly observed that PAN and shellac blends form miscible blends with smooth cross section and one phase figure. The shellac particles were dissolved in DMF with PAN so well that the particles of shellac are not visible in SEM images. The blend morphologies are also very critical in the performance and compatibility of polymers. PAN/SH10 and PAN/SH40 samples show more bumpy and rougher morphology than that of samples with lower shellac concentration than 10 wt%. These two cases indicate shellac aggregation due to excessive shellac incorporation resulted to immiscible blends between PAN and shellac. However, the PAN film with 5 wt% of shellac looks more uniform which is very close to the image of the neat PAN.

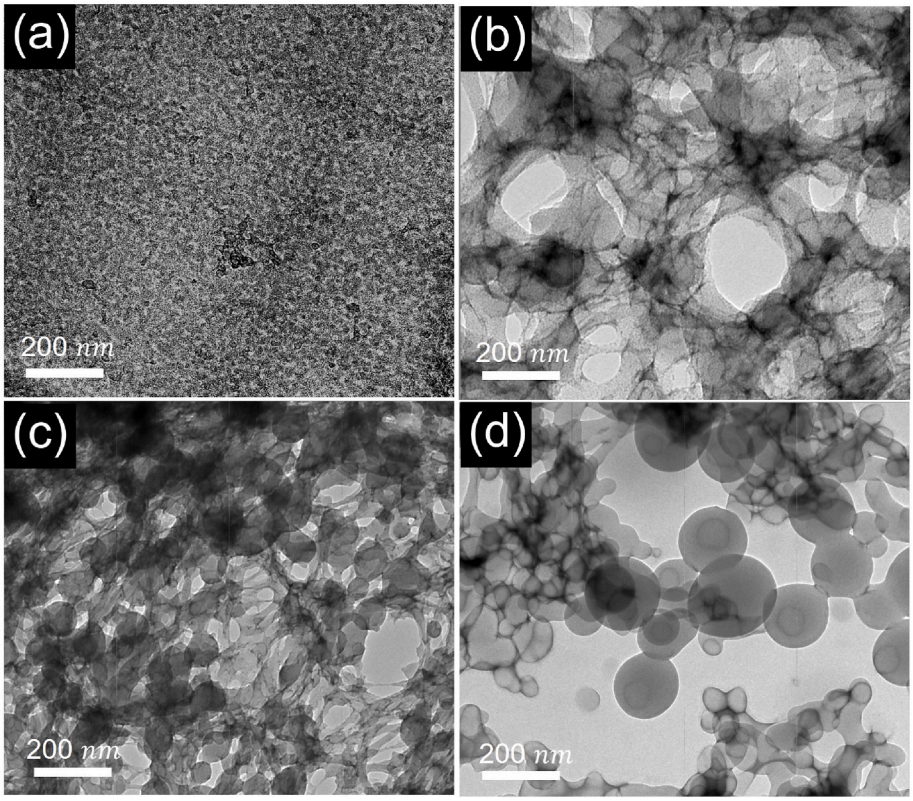

Fig. 4. TEM images of PAN/shellac blends film with different shellac concentration: (a) 0 wt%; (b) 5 wt%; (c) 40 wt%; and (d) 100 wt%, respectively. Macroscopically phase-separated bilayer structure with dark circle-type morphology corresponding to shellac domains.

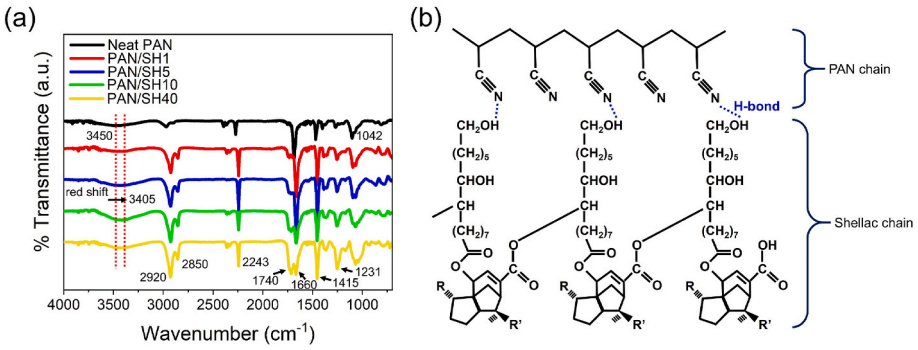

Fig. 5. (a) shows FTIR spectra of PAN/shellac blends with different shellac concentration. (b) the chemical interaction between PAN and shellac chain through hydrogen bonding describing as blue dotted line. (For interpretation of the references to colour in this figure legend, the reader is referred to the Web version of this article.)

Table 2
Band assignments of PAN/shellac blends film obtained from FTIR spectra.

Band (cm^{-1})	Assignments
1042, 1231	Alkoxy CO, epoxy CO
1415	O − H deformation
1660, 1740	C = O stretching of PAN, shellac
2243	C ≡ N stretching
2850 − 2920	C − H stretching
3000 − 3500	N − H stretching

Interestingly, as shown in Fig. 3 (a'-e'), the pore structure or rough surface are not shown in shellac 5 wt% case as well as neat PAN. This sample has stable blending behavior between shellac and PAN chain without significant aggregation and smooth surface causing better affinity between shellac and PAN, and it may leads to enhance interfacial interaction, mechanical strength. As shellac load increases to 40 wt %, shellac are obviously locally aggregated in PAN matrix showing pore structure.

In addition, the negative staining TEM analysis was conducted to investigate miscibility of shellac into the PAN. In the TEM images, a neat PAN sample shows homogeneous one phase structure, however, a blended sample, which includes 40 wt% of shellac concentration, exhibits a segregated structure with PAN-rich phases, where circle-type domains of shellac are observed in the PAN phase (Fig. 4 (a and c)). Furthermore, the circle structures of shellac remarkably are well observed in the sample which is 100% shellac case as shown in Fig. 4 (d). Interestingly, the TEM image of the PAN/SH5 blends shows no apparent contrast on the nanoscale inside the blend sample (Fig. 4 (b)). This clearly demonstrates the homogeneous blending of the shellac at the

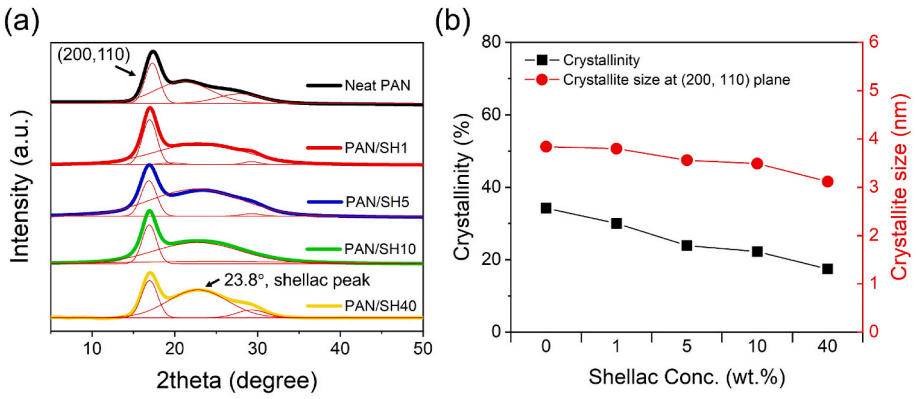

Fig. 6. (a) WAXD patterns of PAN/shellac blends film showing characteristic peaks at around 17 ° (200, 110) plane corresponding to PAN peak, (b) shows crystallinity and crystalline size corresponding to the (200, 110) reflection plane of the PAN film with different shellac concentration obtained from WAXD patterns.

Table 3
Crystallization properties of the (200, 110) reflection in PAN/shellac blends film with different shellac concentration based on WAXD analysis.

	Neat PAN	PAN/SH1	PAN/SH5	PAN/SH10	PAN/SH40
CI (%)	34.2	30.1	23.9	22.2	17.4
2 θ (200, 110)	17.27	16.96	16.85	16.91	16.93
FWHM (200, 110)	2.24	2.19	2.39	2.17	2.25
Crystallite size, H (nm)	3.84	3.8	3.56	3.49	3.12

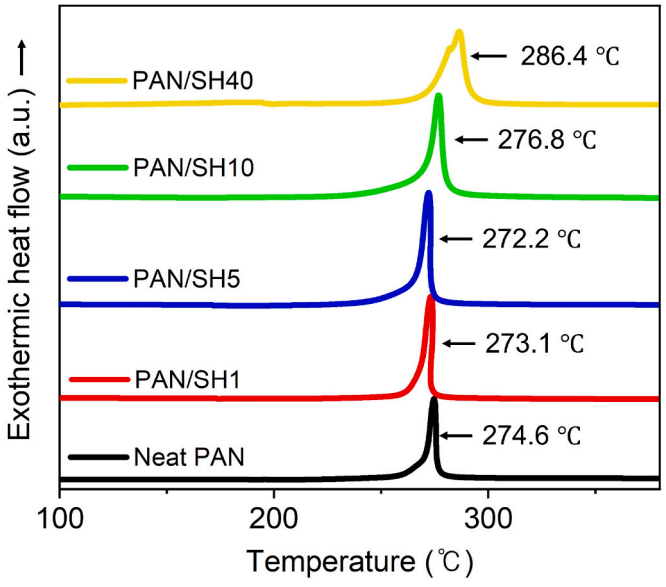

Fig. 7. Non-isothermal DSC scans of PAN/shellac blends film with different shellac concentration.

molecular level compared with PAN/SH40 case having excessive shellac concentration. Note that the excessive shellac addition to the PAN molecules can cause macroscopically phase-separated polymers. Therefore, all these results indicate that optimal concentration of shellac in the PAN blending film is 5 wt% showing successfully molecular-level mixing of PAN and shellac.

3.3. Structural analysis of PAN/shellac blend film

FT-IR spectra of PAN/shellac film was investigated to compare the interaction between PAN and shellac chains (Fig. 5 (a)). One of the important peaks is the band at 2243 cm^{-1} which corresponds to C ≡ N bond as listed in Table 2. Furthermore, the two characteristic peaks at 1660 cm^{-1} and 1740 cm^{-1} correspond to C═O stretching of PAN and shellac, respectively. C═O stretching of PAN may be due to residual DMF solvent in the PAN film. Meanwhile, the intensity of peak at 1740 cm^{-1} increases with increases of shellac concentration meaning that many C═O functional groups are introduced in blends from shellac chain. The C − H stretching peaks are observed in the range of 2850 − 2920 cm^{-1} and the intensity of the peaks increase with increasing of shellac concentration. Furthermore, as shellac content increases, the intensity of peak at 1415 cm^{-1} increases indicating the abundant functional groups of the shellac molecules that can contribute the formation of hydrogen bonding between PAN and shellac. The broad peak in between 3000 cm^{-1} and 3500 cm^{-1} is ascribed to N − H stretching and O − H stretching vibration in PAN and shellac, respectively. Especially, the characteristic peak at 3450 cm^{-1} corresponds to hydrogen bonded N − H. The peak of N − H showed a red shift (meaning peak shift to low wavenumber), indicating that the introduction of shellac could increase the number of O–H groups in molecules and led to the gradual formation of N − H hydrogen bonds with C ≡ N groups in PAN as shown in Fig. 5 b. Meanwhile, Fig. S2 (a) shows FT-IR spectra of neat shellac film to investigate the chemical structure of shellac. There are broad band between 3100 − 3400 cm^{-1} correspond to O − H stretching [27]. Additionally, other strong intensity peaks at 2853 and 2930 cm^{-1} were observed due to the strong symmetric and asymmetric stretching of CH_2, respectively. The peak at 1712 cm^{-1} can be attributed to the C═O stretching of ester of shellac [28]. The weak bands of the shellac can be shown to peak at 1636 cm^{-1} (C═C stretching vibration), 1412 cm^{-1} (−CH_2), 1250 cm^{-1} (C − O stretching), and 1050 cm^{-1} (C − C stretching), respectively [29].

As shown in Fig. 6, the WAXD patterns of the PAN/shellac blend films were displayed. The representative peak at ~17 ° is ascribed to the (200,110) planes of PAN. As the shellac content increases to 5 wt%, the peak shifts down from 17.27 ° (Neat PAN) to 16.85 ° (PAN/SH5) as listed in Table 3. When shellac content further increases to 10 wt% and 40 wt%, the peak back to 16.91 ° and 16.93 °, respectively. The down shift of PAN peak of the PAN/SH5 film suggests that the PAN crystalline packaging becomes loose. The well dissolved shellac chains could become entangled with PAN chains, and thus distort the PAN crystalline structures showing decreases in crystallinity of the PAN film from 34.2 to 17.4 by introducing of shellac and increasing content by 40 wt% as shown in Table 3. While shellac become phase separated at a concentration of 10 wt%, the PAN peak shifts back to the original position, since there are limited interactions between PAN and shellac chains

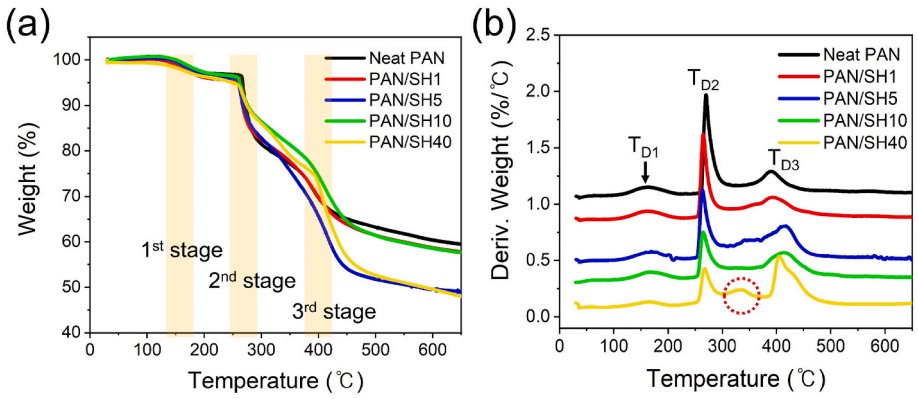

Fig. 8. (a) TGA thermographs, (b) derivative curve of PAN/shellac blends film with different shellac concentration.

Table 4
Thermal degradation temperature and 5 wt% loss temperature of PAN/shellac blends film with different shellac concentration.

Sample	T_{D1}	T_{D2}	T_{D3}	5% weight loss temperature, $T_D^{5\%}$ (°C)
Neat PAN	163.22	269.93	389.77	267.25
PAN/SH1	162.05	264.93	391.81	260.49
PAN/SH5	168.59	263.36	415.65	259.75
PAN/SH10	166.28	264.51	415.20	262.08
PAN/SH40	162.18	267.24	404.74	250.64

once phase separation occurs. Furthermore, the PAN peak intensity also decreases as shellac content increases compared with neat PAN case, relatively. On the other hand, the shellac peaks at 23.8 °, which are ascribed to the crystal peak, show higher intensity than that of neat PAN as shown in Fig. 6 (fitted peak). Accordingly, the crystallite size of the PAN chain also decreases as shellac was incorporated in PAN, subsequent decreases gradually as shellac concentration increases. Meanwhile, the crystallinity and crystallite size of only shellac film showing the characteristic peak at 18.6 ° are 6.1% and 1.31 nm, respectively (Fig. S1).

3.4. Thermal properties of PAN/shellac blend film

Fig. 7 shows the DSC curves of PAN/shellac films. PAN exhibits a strong exothermic peak, which is attributed to both cyclization and oxidation reactions. The initiation temperature of neat PAN is around 270 °C due to the presence of ester comonomers, which need higher activation energy for cyclization. Meanwhile, the exothermic peak shift to low temperature slightly and peak area becomes narrower with the addition of shellac in PAN compared with that of neat PAN. It indicates shellac molecules can be blended with PAN molecules leading one phase structure from high miscibility. Furthermore, probably, shellac segments and PAN chain could exert interaction and the interaction facilitates to destroy the crystallinity of the PAN chain, suggesting that the decrease of the crystallization temperature of the PAN chain in the PAN/shellac blends film by the introduction of shellac segments. However, the peak shift to right of high temperature beyond 5 wt% of shellac. In accordance with, Fig. S2 (b), shows the exothermic behavior of neat shellac at 2nd cooling scans indicating convex exothermic curve around 60 °C, but there is no crystallization peak. As a result, PAN stabilization can be conducted at lower temperature, which can contribute to lowering the production cost.

The thermal degradation behavior of the PAN/shellac blends was investigated via TGA to compare the effect of shellac incorporation in the PAN. As shown in Fig. 8, normally, there are 3 areas of weight loss. The first weight loss observed in the range 160 – 170 °C relates to water or solvent present in the sample. The second weight loss observed in the range of 250 – 300 °C, PAN started to decompose from the blend film, which is in-line with the initiating temperature in the DSC thermogram. In this degradation part, the C ≡ N bonds are broken resulting in cyclization or stabilization from PAN chain. The third weight loss can be found between 350 °C and 420 °C, which is attributed to the degradation and produces lots of volatile particles. Especially, the PAN film with 40 wt% of shellac shows additional degradation peak around 335 °C, which relates to structural decomposition of the shellac resulting from the excessive shellac concentration. As shown in Fig. S2 (c and d), TGA curve of neat shellac indicates 3 areas of weight loss first weight loss in the range of 35 – 150 °C relates to water or solvent present, second weight loss in the range of 250 – 450 °C relates to the structural decomposition of the shellac. Above 500 °C, the shellac has been converted fully to TRGO. Furthermore, there is a specific degradation peak around 365 °C corresponding to shellac decomposition as evidence of

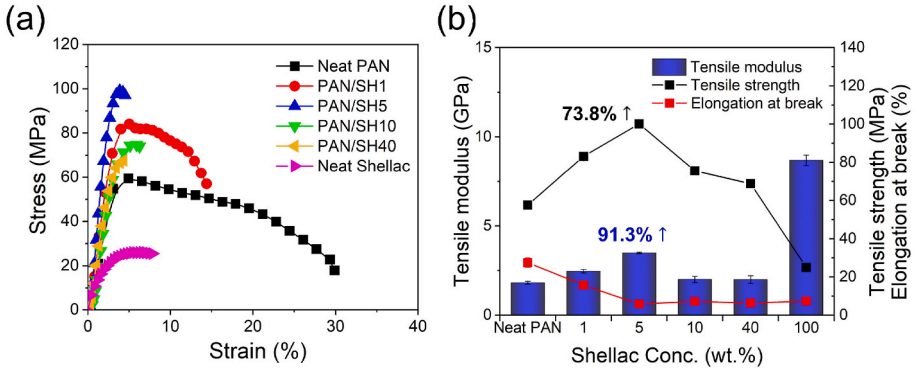

Fig. 9. (a) Tensile stress-strain curves and (b) tensile strength, modulus and elongation at break of PAN/shellac blends film with different shellac concentration.

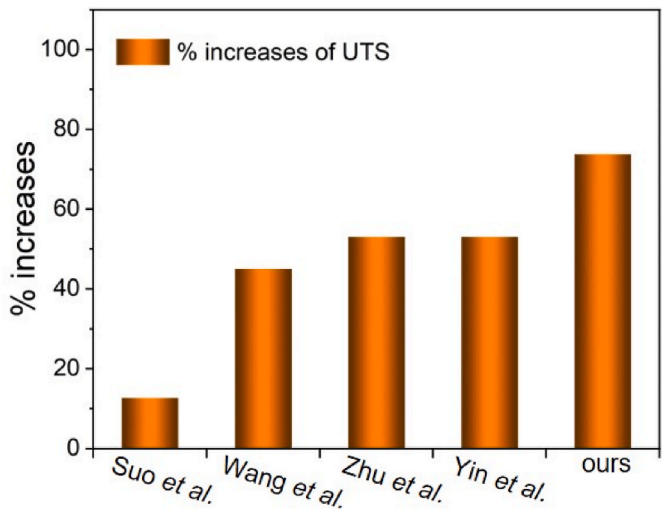

Fig. 10. Comparison of percentage increases in the ultimate tensile strength (UTS) of PAN/polymer blends film with previous reports.

the additional peak of the PAN/SH40 case (Fig. 8 (b)).

Meanwhile, the thermal stability of PAN/shellac film decreases as shellac content increases showing decreases of temperature of 5% weight loss as listed in Table 4, whereas, neat shellac has low temperature of 5% weight loss around 200 °C. Furthermore, the major degradation temperature (T_{D2}) of each blend is listed in Table 4. The onset temperature for shellac decomposition of each sample differs so the thermal stability of the PAN changes according to the shellac stability. PAN/SH5 show the lowest degradation temperature meaning the low thermal stability. It is consistent with the results of the DSC analysis. As further studies, carbonization behavior will be investigated at higher temperature for fabricating of carbon fiber.

3.5. Mechanical performance of PAN/shellac blend film

The effects of compatibility of PAN/shellac blends on the mechanical properties of the films were investigated through tensile test via DMA equipment. The stress-strain curves of PAN/shellac films are shown in Fig. 9 and Table S1. Interestingly, the PAN/SH5 case exhibits the highest tensile strength and modulus of 100 MPa, 3.5 GPa, respectively, which increased by 73.8%, 91.3% compared with that of neat PAN film (57.6 MPa, 1.8 GPa). However, at a higher shellac content, such as 10 wt% and 40 wt%, the tensile strengths of the films are 75 MPa and 68 MPa, respectively, which are higher than neat PAN, but lower than that of SH5 case. These results are consistent with DMA behavior as shown in Fig. 10. It may be due to the molecular structure of shellac containing hard and soft segments as well as phase separation in the PAN/shellac blends resulted from excessive shellac concentration. Therefore, it can be argued that the tensile properties of the PAN film could be affected by shellac concentration and chain blends. Furthermore, the tensile properties of neat shellac film were analyzed to compare with that of PAN/shellac blends film. As shown in Fig. 9 and Table S1, the tensile strength of neat shellac is 25 MPa, which the lowest value of all samples, whereas, the tensile modulus has the highest value of 8.7 GPa resulted from high stiffness and brittleness of shellac. Accordingly, it can be confirmed that the addition of shellac to the PAN matrix can enhance modulus as well as strength due to the enhanced compatibility with optimal concentration of shellac into the PAN matrix.

Meanwhile, as shown in Fig. 10, the increase in the tensile strength of the presently investigated PAN/shellac blends film were compared with previously published results for PAN/polymer blends composites. Suo et al. reported that addition of 0.5 wt% of thermoplastic polyurethane (TPU) to the PAN enhanced the tensile strength by 12.7%, when compared to the control sample [30]. Wang et al. reported that PAN/-polyimide (PI) bilayer films with enhanced the tensile strength by 45% [31]. Zhu et al. prepared PAN/poly(vinyl alcohol) (PVA) blends film by solution casting and reported a 53% increase in the tensile strength [32]. In addition, Yin et al. reported that the introduction of attapulgite (AT) 1 wt% into the PAN also improved the tensile strength by 53% [33]. However, in this study, tensile strength of the PAN/shellac blends film was improved by 73.8%, significantly higher than those reported previously.

Dynamic mechanical analysis was conducted to understand the viscoelastic behavior of the PAN/shellac films with regard to change in temperature (Fig. 11, Table S2). The storage modulus can be related to Young's modulus measured during static test. The loss modulus value is related to modulus values in the viscous portion. Tan delta is the loss factor meaning the ratio of loss modulus over storage modulus. It was observed that shellac does not deteriorate PAN properties. When 1 wt% of shellac was added to PAN, E' increases due to purity difference of the shellac meaning higher blending performance and compatibility between shellac and PAN. For 5 wt% of shellac, the E' increases by 60% compared with that of neat PAN, furthermore, with further increases of shellac content to 10 wt% and 40 wt%, the stiffening of PAN/shellac films becomes weaker showing 57% and 32% increases of E' for PAN/SH10 and PAN/SH40, respectively. The stress transfer can be caused by more rigid shellac molecules and strong interfacial adhesion between PAN and shellac chains. On the other hand, the tan delta values decrease gradually with increases of shellac content in PAN meaning enhanced elastic properties as well as lower damping properties of the blends film. Meanwhile, Fig. 11 (b) shows that glass transition temperature, T_g increases slightly with increasing of shellac concentration. The up-shift T_g

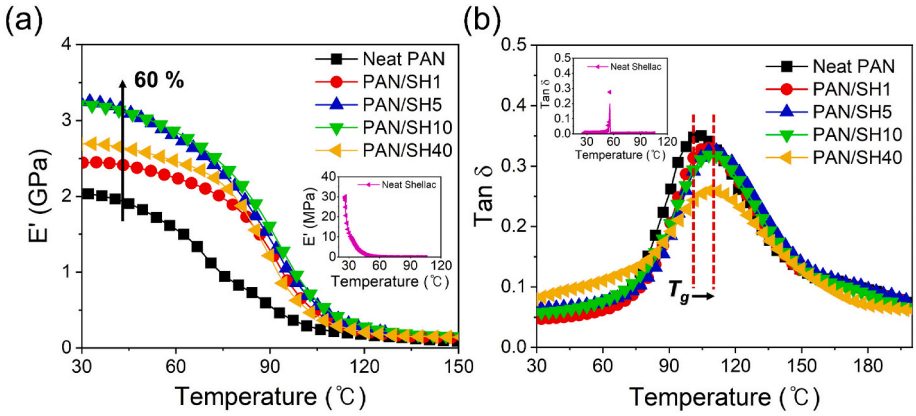

Fig. 11. (a), (b) show the storage modulus and tan δ of PAN/shellac film with different shellac concentration. Inset graphs show storage modulus and tan δ of neat shellac film in the (a) and (b), respectively.

suggests that the interaction between PAN and shellac chains in PAN/SH5 case are more effective than the others. Furthermore, the dynamic mechanical behavior of neat shellac film was investigated to compare with that of PAN/shellac blends film. As shown in Fig. 11 and Table S2, the storage modulus of neat shellac is 30 MPa, whereas, the tan delta peak intensity is 0.27 where at T_g of 55.6 °C.

4. Conclusion

Blends of PAN and shellac, which is biomass-polymer and new carbon source material, were produced through simple solution casting method. In this study, the compatibility of miscibility between PAN and shellac was investigated and the optimal ratio of that was determined to be used as a novel biomass carbon fiber precursor. From the detailed FT-IR, the optimal concentration of shellac in terms of hydrogen bonding between hydroxyl groups of shellac and C ≡ N groups of PAN was determined to be 5 wt%. Furthermore, PAN/SH5 film showed the lowest degradation temperature meaning the low thermal stability. The PAN/shellac blends film exhibited outstanding mechanical performances resulting from the superior chain compatibility between PAN and shellac. In addition, the blends film exhibited 73.8% higher tensile strength (100 MPa), compared to the neat PAN. Moreover, the blends film exhibited the highest *E'* (3.26 GPa, 60% improvement). This study is the first attempt to make polymer shellac blends with PAN chain to be used for carbon fiber precursor. These new findings will open new ways to understand the novel biomass-based carbon fiber manufacturing. This study can be further carried with carbon fiber precursor, PAN and moreover that polymer blend can be spun to fiber and formed into carbon fiber via the carbonization process. Furthermore, this study demonstrated a new application area of shellac which is rising material in biomass industries. The most important finding of this research was to find a potential replacement of PAN with a biodegradable polymer and making the PAN precursor greener technology to improve the globe environment.

Authorship statement

Beom-Gon Cho: Investigation, Writing-Original draft preparation.
Jung-Eun Lee: Formal analysis.
Seung-Yeol Jeon: Methodology, Funding acquisition.
Han Gi Chae: Methodology, Supervision, Funding acquisition, Writing-review & editing.

Declaration of competing interest

The authors declare that they have no known competing financial interests or personal relationships that could have appeared to influence the work reported in this paper.

Data availability

Data will be made available on request.

Acknowledgements

This research was financially supported by National Research Foundation (NRF) and fundamental research assignment funded by the Ministry of Science and ICT of Korea (Grant No. 2021R1A2C200440411) and Korea Automotive Technology Institute (Grant No. II51731), respectively.

Appendix A. Supplementary data

Supplementary data to this article can be found online at https://doi.org/10.1016/j.polymertesting.2023.107983.

References

[1] I. Fortelny, J. Juza, The effects of copolymer compatibilizers on the phase structure evolution in polymer blends-A review, Materials (2021) 14.
[2] M.E. Mendoza-Duarte, I.A. Estrada-Moreno, P.E. Garcia-Casillas, A. Vega-Rios, Stiff-elongated balance of PLA-based polymer blends, Polym. Bull. (Berlin) 13 (2021).
[3] K. Muller, D. Van Opdenbosch, C. Zollfrank, Cellulose blends with polylactic acid or polyamide 6 from solution blending: microstructure and polymer interactions, Mater. Today Commun. 30 (2022).
[4] T.C. O'Connor, T. Ge, G.S. Grest, Composite entanglement topology and extensional rheology of symmetric ring-linear polymer blends, J. Rheol. 66 (2022) 49–65.
[5] Y. Zhao, Z. Lu, H.L. Yao, J. Zhang, X.Z. Yuan, Y.Y. Cui, Y.P. Nie, Development and mechanical properties of HDPE/PA6 blends: polymer-blend geocells, Geotext. Geomembranes 49 (2021) 1600–1612.
[6] B. Hexig, H. Alata, N. Asakawa, Y. Inoue, Generation of compositional-gradient structures in biodegradable, immiscible, polymer blends by intermolecular hydrogen-bonding interactions, Adv. Funct. Mater. 15 (2005) 1630–1634.
[7] H. Huang, Y. Hu, J.M. Zhang, H. Sato, H.T. Zhang, I. Noda, Y. Ozaki, Miscibility and hydrogen-bonding interactions in biodegradable polymer blends of poly(3-hydroxybutyrate) and a partially hydrolyzed poly(vinyl alcohol), J. Phys. Chem. B 109 (2005) 19175–19183.
[8] P. Tipduangta, P. Belton, W.J. McAuley, S. Qi, The use of polymer blends to improve stability and performance of electrospun solid dispersions: the role of miscibility and phase separation, Int. J. Pharm. (Amst.) (2021) 602.
[9] S. Viswanathan, M.D. Dadmun, Optimizing hydrogen-bonding in creating miscible liquid crystalline polymer blends by structural modification of the blend components, Macromolecules 36 (2003) 3196–3205.
[10] A. Sionkowska, Current research on the blends of natural and synthetic polymers as new biomaterials: review, Prog. Polym. Sci. 36 (2011) 1254–1276.
[11] S. Tabasum, M. Younas, M.A. Zaeem, I. Majeed, M. Majeed, A. Noreen, M.N. Iqbal, K.M. Zia, A review on blending of corn starch with natural and synthetic polymers, and inorganic nanoparticles with mathematical modeling, Int. J. Biol. Macromol. 122 (2019) 969–996.
[12] R.N. Tiozon, A.P. Bonto, N. Sreenivasulu, Enhancing the functional properties of rice starch through biopolymer blending for industrial applications: a review, Int. J. Biol. Macromol. 192 (2021) 100–117.
[13] M. Younas, A. Noreen, A. Sharif, A. Majeed, A. Hassan, S. Tabasum, A. Mohammadi, K.M. Zia, A review on versatile applications of blends and composites of CNC with natural and synthetic polymers with mathematical modeling, Int. J. Biol. Macromol. 124 (2019) 591–626.
[14] E. Frank, F. Hermanutz, M.R. Buchmeiser, Carbon fibers: precursors, manufacturing, and properties, Macromol. Mater. Eng. 297 (2012) 493–501.
[15] X.S. Huang, Fabrication and properties of carbon fibers, Materials 2 (2009) 2369–2403.
[16] B. Wang, Y. Ma, B. Na, R.H. Lv, H.S. Liu, W.P. Li, H.Y. Zhou, Enhanced dielectric thermal stability and permittivity of flexible composite films based on BaTiO3 nanoparticles highly filled PVDF/PAN blend nanofibrous membranes, Polym. Compos. 39 (2018) E1841–E1848.
[17] H.C. Jeffrey Luo, Amir A. Bakhtiary Davijani, H. Clive Liu, Po-Hsiang Wang, Robert J. Moon, Satish Kumar, Influence of high loading of cellulose nanocrystals in polyacrylonitrile composite films, Cellulose 24 (2017) 1745–1758.
[18] B.G. Cho, S.R. Joshi, J.H. Han, G.H. Kim, Y.B. Park, Interphase strengthening of carbon fiber/polyamide 6 composites through mixture of sizing agent and reduced graphene oxide coating, Composer Part a-Appl S 149 (2021).
[19] B.G. Cho, S.R. Joshi, J. Lee, Y.B. Park, G.H. Kim, Direct growth of thermally reduced graphene oxide on carbon fiber for enhanced mechanical strength, Compos. B Eng. 193 (2020).
[20] B.G. Cho, S.R. Joshi, S.J. Lee, S.K. Kim, Y.B. Park, G.H. Kim, Enhanced mechanical and antibacterial properties of nanocomposites based on poly(vinyl alcohol) and biopolymer-derived reduced graphene oxide, Polym. Bull. (Berlin) 13 (2021).
[21] K. Li, H. Zheng, H. Zhang, W.W. Zhang, K. Li, J. Xu, A novel approach to the fabrication of bleached shellac by a totally chlorine-free (TCF) bleaching method, RSC Adv. 6 (2016) 55618–55625.
[22] Y.N. Singhbabu, S.K. Choudhary, N. Shukla, S. Das, R.K. Sahu, Observation of large positive magneto-resistance in bubble decorated graphene oxide films derived from shellac biopolymer: a new carbon source and facile method for morphology-controlled properties, Nanoscale 7 (2015) 6510–6519.
[23] A. Mondal, M.A. Sohel, A.P. Mohammed, A.S. Anu, S. Thomas, A. SenGupta, Crystallization study of shellac investigated by differential scanning calorimetry, Polym. Bull. 77 (2020) 5127–5143.
[24] Y.N. Singhbabu, B. Sivakumar, S.K. Choudhary, S. Das, R.K. Sahu, Corrosion-protective reduced graphene oxide coated cold rolled steel prepared using industrial setup: a study of protocol feasibility for commercial production, Surf. Coating. Technol. 349 (2018) 119–132.
[25] Y. He, B. Zhu, Y. Inoue, Hydrogen bonds in polymer blends, Prog. Polym. Sci. 29 (2004) 1021–1051.
[26] Y. Kobori, R. Yasumitsu, I. Akiba, S. Akiyama, H. Sano, Interfacial Irregularity Induced by Hydrogen Bonds at the Interface in Immiscible Polymer Blends, E-Polymers, 2004.
[27] M.A.K.M. Aslam, Z.A. Raza, Polyvinyl alcohol: a review of research status and use of polyvinyl alcohol based nanocomposites, Polym. Eng. Sci. 58 (2018) 2119–2132.
[28] T.M.P.K.V. Ravi, S. Ramaiah, Novel colon targeted drug delivery system using natural polymers, Indian J. Pharmaceut. Sci. 70 (2008) 3.

[29] H.Z.K. Li, H. Zhang, W.W. Zhang, K. Li, J. Xu, A novel approach to the fabrication of bleached shellac by a totally chlorine-free (TCF) bleaching method, RSC Adv. 6 (2016) 55618–55625.
[30] X. Suo, Z. Cao, Y. Yu, Y. Liu, Dynamic self-stiffening in polyacrylonitrile/thermoplastic polyurethane composites, Compos. Sci. Technol. (2020) 198.
[31] X. Wang, C. He, L. Luo, D. Chen, X. Liu, J. Qin, A fast response, large deformation, excellent mechanical pH-responsive polyacrylonitrile/polyimide bilayer film, Polymer (2020) 191.
[32] G. Zhu, F. Wang, K. Xu, Q. Gao, Y. Liu, Study on properties of poly(vinyl alcohol)/polyacrylonitrile blend film, Polímeros - Ciência Tecnol. 23 (2013) 146–151.
[33] H. Yin, H. Chen, D. Chen, Morphology and mechanical properties of polyacrylonitrile/attapulgite nanocomposite, J. Mater. Sci. 45 (2010) 2372–2380.